Materials Research Express

PAPER

Frequency and density dependencies of the electromagnetic parameters of carbon nanotube and graphene nanoplatelet based composites in the microwave and terahertz ranges

Materials Research Express

PAPER

Frequency and density dependencies of the electromagnetic parameters of carbon nanotube and graphene nanoplatelet based composites in the microwave and terahertz ranges

RECEIVED
20 May 2019

REVISED
5 June 2019

ACCEPTED FOR PUBLICATION
3 July 2019

PUBLISHED
10 July 2019

M V Shuba[1,2], D I Yuko[1], G Gorokhov[1], D Meisak[1], D S Bychanok[1,2], P P Kuzhir[1,2], S A Maksimenko[1,2], P Angelova[3], E Ivanov[3] and R Kotsilkova[3]

[1] Institute for Nuclear Problems, Belarus State University, Bobruiskaya 11, 220050 Minsk, Belarus
[2] Tomsk State University, Lenin Avenue 36, 634050, Tomsk, Russia
[3] OLEM, Institute of Mechanics Bulgarian Academy of Sciences, Acad. G. Bonchev str. 4, Sofia, 1113, Bulgaria

E-mail: mikhail.shuba@gmail.com

Keywords: carbon nanotube, graphene platelet, composite, effective conductivity, microwave and terahertz conductivity

Abstract

Frequency and density dependencies of the effective conductivity and permittivity of carbon nanotube (CNT) and graphene nanoplatelet (GNP) based polymer composites are studied in the microwave (0.1–20, 26–36 GHz) and terahertz (0.2–1.0 THz) ranges. Strong frequency dependencies of the effective conductivity are associated with the screening effect occurred in individual nanoparticles and their agglomerates. Density dependencies are fitted with power-law formulas with frequency dependent exponents. Thin films comprising the CNTs or GNPs were proposed to consider as 'perfect' composites with the maximal possible electromagnetic interaction of the inclusions. Comparison between films and polymer composites has been done. The ratio of the microwave to terahertz conductivities of the composite is proposed to estimate the efficacy of GNP interaction with the electromagnetic field. Synergy effect in the enhancement of the effective microwave conductivity is demonstrated for the composite comprising a mixture of CNTs and GNPs.

The inclusion of conductive nanoparticles into dielectric polymer matrix leads to the formation in it of conductive pathways so that the composite material becomes conductive itself. Percolation theory introduces a percolation threshold p_c—a minimal concentration of a filler needed to transfer the material from insulating to conducting state [1]. The value p_c strongly depends on the aspect ratio of the filler (nano-) particles and their distribution in the polymer matrix [2, 3].

Composite materials with carbon nanotubes (CNTs) and graphene nanoplatelets (GNPs) as inclusions have been actively studied for two past decades, see e.g. [4–10]. Many efforts have been made to reach low percolation threshold which typically lays in the ranges ~0.002 − 1%, ~0.02 − 1%, and ~0.1 − 6 % for single-walled CNT (SWCNT), multi-walled CNT (MWCNT), and GNP based composite, respectively [7, 11, 12]. The concentration dependence of the static electrical conductivity above the percolation threshold for a 3D CNT network has been shown to follow the power-law with the exponent in the range (1, 4) peaking at about 2 [4].

The concentration dependence of the effective conductivity σ_{eff} of CNT and GNP based composites in the high-frequency range is not the same as in the static regime. The broadband spectroscopy study [6, 13, 14] carried out for both GNP and CNT composites has shown that the effective conductivity in the microwave and terahertz ranges is several orders higher than that in the static regime even at high filler loading (e.g., at 4 wt%, that is above the percolation threshold). The difference could be mainly due to two reasons: (i) some inclusions are not involved in conductive network of the composite, so that they contribute into dynamic but not into static effective electrical conductivity; (ii) the contact resistance between inclusions contributes much weaker to the dynamic effective conductivity than to the static one.

It should be noted that the intrinsic conductivity of the carbon inclusions is almost frequency independent below 1 THz and it follows the Drude law [15, 16] with the relaxation time being typically less than 100 fs. For

example, for SWCNTs of high crystalline quality, it is found that $\tau \approx$ 60–100 fs at room temperature in the range 0.2–1.0 THz [17, 18]. So, the mean free path of the electrons on the Fermi level is less than 100 nm in SWCNTs, and it is much less than typical tube length (>500 nm). That is also true for MWCNTs and GNPs as they are more defective than SWCNTs, for example, it was found that $\tau = 26$ fs for reduced graphene oxide in the terahertz range [19].

Since the intrinsic conductivity of inclusions practically does not depend on frequency f, one may conclude that the effective field within each nanoparticle strongly depends on the frequency. As discussed in [20, 21], the screening effect within CNTs or their agglomerates is the main mechanism that leads to a strong frequency dependence of $\sigma_{\text{eff}}(f)$. Screening effect appears as a result of the compensation of the incident field by the depolarizing field of the inclusion. The effect is stronger at lower frequencies and for smaller size nanoparticles [20, 22]. It weakens when particles form a conductive network that is similar, in some respect, to an increase of the effective particle sizes. In this paper, we demonstrate that namely, the screening effect is the main mechanism which determines frequency dependence of the effective conductivity of both GNP and CNT composites. We compare the electromagnetic response of CNT and GNP composites and show that the screening effect appears to be stronger in the GNPs than in the CNTs for our samples.

The broadband conductivity spectra [6, 13, 14] also demonstrate that the dependence of σ_{eff} on the filler concentration gets weaker as frequency increases. Very few papers analyze the concentration dependence of σ_{eff} for CNT and GNP composites in the microwave and terahertz ranges. Recently, it has been shown that the concentration dependence at 30 GHz follows the power-law with the exponent β being in the range 1.7 ± 0.1 and 2.0 ± 0.2 for MWCNT and SWCNT sponges, respectively [23], and $\beta = 1.3$ for hybrid films comprising SWCNTs and WS_2 nanotubes [17]. In the terahertz range, the exponent is found to be close to unity [17, 24]. At frequency 1MHz, the concentration dependence of the conductivity of MWCNT polymer composite has been also fitted with power-law with the exponent ≈0.4 [25]. Here, we demonstrate the power-law dependence of the conductivity on the filler concentration for CNT and GNP composites in a wide frequency range from 100 MHz up to 1 THz. We also propose to determine GNP concentration from the terahertz measurements, in the same manner as it has been done for CNT composites [17, 24, 26].

1. Material and preparation technique

In our work, the poly(lactic) acid Ingeo PLA 3D850 from Nature Works, USA was used as a matrix polymer. Graphene nanoplatelets (TNGNPs), MWCNTs (TNIMH4) and industrial grade of graphene nanoplatelets (TNIGNPs) were supplied from Times Nano, Chengdu, China. TNIGNPs have a number of graphene layers less than 30; the size of the platelets is 2–16 μm. Hereinafter, we shall call this material as large-size GNPs. We shall call TNGNPs as small-size GNPs, as they have a smaller size of platelets (5–10 μm) and the number of graphene layers (<20). MWCNTs have outer diameter 10–30 nm, inner diameters 5–10 nm, length 10–30 μm and purity >95%.

To fabricate polymer composite, the PLA pellets and fillers were dried and melt mixed in twin screw extruder in the temperature range 170 °C–180 °C and a screw speed of 40 rpm. Two masterbatches of 6 wt% TNIGNPs and 6 wt% MWCNTs were prepared by one extrusion run. Then, the masterbatches were diluted by extrusion with the neat PLA to produce mono-filler composites of 1.5 and 3 wt% filler contents, as well as bi-filler composites with various proportions of both fillers. Details of sample characterization with the electron microscopy, rheological methods, and dielectric and Raman spectroscopy are presented in [27, 28]. The samples and their static conductivities are collected in table 1.

CNT films were prepared via the vacuum filtration technique [29]. Briefly, a MWCNT material was dispersed by ultrasonic treatment (Ultrasonic device UZDN-2T, 44 kHz, maximum power) for 1 h in an aqueous suspension with 1 wt% sodium-dodecylsulfate. The suspension of CNTs was centrifuged at 1000 g for 20 min and then it was filtrated through a cellulose nitrate membrane filter (0.2 μm pore size, the thickness of 100 μm) causing a CNT film to collect on the filter. The obtained film was washed with distillate water to remove the surfactant. The filter was then dissolved with acetone and the film was transferred on the 10 μm-thick poly-tetrafluoroethylene (PTFE) substrate for terahertz and microwave measurements.

For the preparation of the GNP film, a GNP material was dispersed by ultrasonic treatment for 10 h in isopropyl alcohol. Immediately after ultrasonication, the suspension was left for 7 h. Heavy and large particles were precipitated and upper part of the suspension with smaller particles was filtered through a filter previously coated with a 3 μm thick film comprising non-conductive inorganic WS_2 nanotubes [30]. This film was prepared with filtration methods as described in [21], it is transparent below 1 THz and plays a role of supporting substrate for GNP film during its transfer onto PTFE substrate. The thicknesses of the CNT and GNP films were in the range 1–2 μm.

Table 1. Samples and their static electrical conductivity.

Sample	σ_{eff} (S/cm)
1.5% GNP	$<10^{-10}$
3.0% GNP	$<10^{-10}$
6.0% GNP	21×10^{-6}
1.5% CNT	$<10^{-10}$
3.0% CNT	4×10^{-6}
6.0% CNT	40×10^{-6}
1.5% GNP + 4.5% CNT	100×10^{-6}
3.0% GNP + 3.0% CNT	74×10^{-6}
4.5% GNP + 1.5% CNT	60×10^{-6}
1.5% GNP + 1.5% CNT	0.026×10^{-6}

Note. Numbers in percents indicate weight fractions of CNTs and GNPs.

Raman spectroscopy was performed using the Raman spectrometer combined with the confocal microscope Nanofinder High End (Tokyo Instruments) with 532 nm laser excitation.

The complex transmission of the samples was measured under normal incidence in the range 0.2–1.0 THz using time-domain terahertz spectrometer (EKSPLA, Vilnius, Lithuania). The sample conductivity was then calculated using the Fresnel equations for dielectric slab [31]. The microwave conductivity measurements in the ranges 0.1–18 GHz and 26–36 GHz were performed by waveguide method [32] using a vector analyzer R4M-18 (MICRAN, Tomsk, Russia) and a scalar network analyzer R2-408R (ELMIKA, Vilnius, Lithuania), respectively. Effective conductivity of the samples in the range 25 Hz—10 MHz was measured with a broadband analyzer 7-28 (MNIPI, Belarus).

2. Results and discussion

Typical scanning electron microscopy (SEM) images of the films comprising small- and large-size GNPs and MWCNTs are represented in figure 1. The difference in size between different GNP samples is clearly seen in figures 1(a), (b). Note also that MWCNTs are curved and their lengths become several micrometers after ultrasonic treatment [33].

Normalized Raman spectra of large- and small-size GNPs are shown in figure 2. The dominant features are a D-band (1320–1350 cm^{-1}), 2D-band (2650–2750 cm^{-1}), and high-frequency G-band (1570–1600 cm^{-1}) [34]. D-band occurs due to disorder-induced symmetry-lowering effects. The 2D-band is an overtone of the D-band due to a two-phonon double-resonant scattering process, and G-band originates from tangential vibrations of sp_2-hybridized carbon atoms. Normalized Raman spectra of large- and small-size GNPs are very similar indicating that the crystalline structure of both materials is the same. The small ratio of the intensity of G-mode to that of the D-mode $I_D/I_G = 0.055$ indicates the high crystalline quality of both samples.

Figure 3 demonstrates frequency dependences of the real parts of the effective permittivity ε_{eff} and conductivity σ_{eff} and dielectric loss tangent $\tan\delta = \text{Im}(\varepsilon_{\text{eff}})/\text{Re}(\varepsilon_{\text{eff}})$ for films comprising large- and small-size GNPs. The differences between the samples are identical to those observed for films comprising short and long CNTs [35]. Namely, (i) the real parts of the conductivity and permittivity and loss tangent are larger for large-size GNPs, and (ii) frequency dependence of the conductivity is stronger for smaller-size GNPs. Thus, we can conclude that the finite-size effect strongly influences the interaction between GNPs and electromagnetic field. Further, we shall consider GNP samples comprising only large-size GNPs, as they show a stronger electromagnetic response.

Figure 4 shows the spectra of the real part of the effective conductivity of CNT/PLA and GNP/PLA composites at different mass fractions of the inclusions. Strong frequency dependence $\text{Re}[\varepsilon_{\text{eff}}(f)]$ at low frequencies (<1 kHz) for GNP/PLA samples at 1.5 and 3 wt% and for CNT/PLA samples at 1.5 wt% indicates the absence of the percolation effect. Very weak frequency dependence $\text{Re}[\varepsilon_{\text{eff}}(f)]$ of other samples below 1 kHz indicates that this sample concentration is above the percolation threshold.

Figure 5 shows the spectra of the real part of the conductivity and permittivity of PLA, CNT film and CNT/PLA composites at different CNT mass fractions. The same spectra are shown in figure 6 for GNP film and GNP/PLA composites. The conductivity of the film and composites both for CNT and GNP samples increases with frequency. Frequency dependence of the conductivity is stronger for the composites with lower weight concentration, and it is the weakest for the films. Qualitatively similar behavior of the conductivity in figures 5 and 6 indicates that the mechanism of electromagnetic interaction could be the same in GNP and CNT samples.

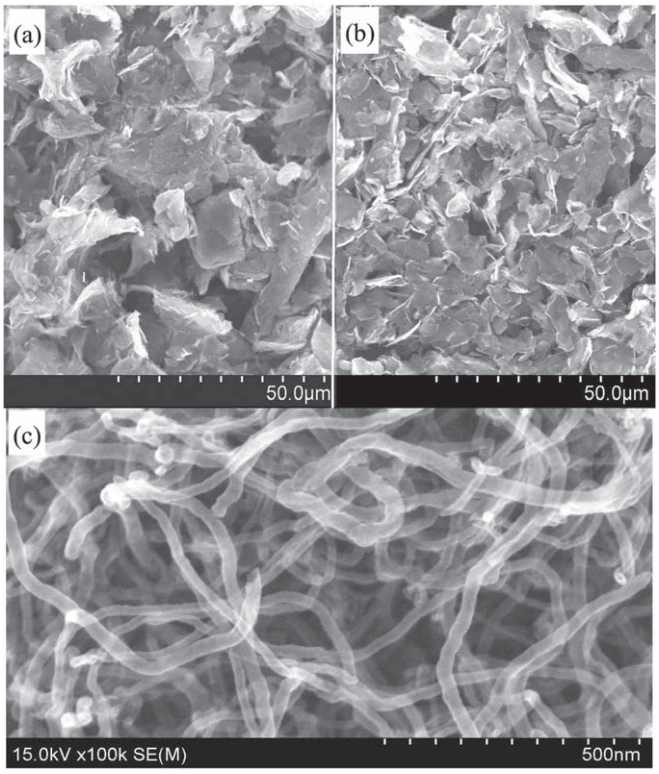

Figure 1. SEM image of the film comprising (a) large- and (b) small-size GNPs and (c) MWCNTs.

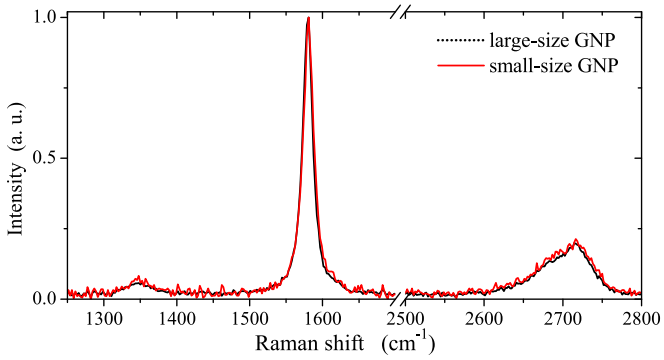

Figure 2. Raman spectra of large- and small-size GNPs.

Indeed, it has been shown that CNT and GNP can be modeled as a spheroid (prolate or oblate) made of anisotropic conducting material [36–39]. This model takes into account the screening effect in individual nanoparticle and qualitatively explains the strong frequency dependence of the effective conductivity of the CNT and GNP composites in the microwave and subterahertz ranges.

Since the intrinsic conductivity of the inclusions practically does not depend on the frequency [15, 19], one can suppose that the effective electromagnetic field within nanoparticles and their agglomerates is smaller than the incident field and it depends on the frequency. Following the paper [21] we associate strong frequency dependence in figures 5 and 6 with the screening effect due to the polarization of the inclusion in the quasi-static regime of its electromagnetic interaction [20, 22]. The screening effect is smaller when particles form a conducting network; this explains the weaker frequency dependence of σ_{eff} for the films than for the composites in figures 5 and 6.

Let us note that the screening effect is weak for long-length CNTs (>1 μm) in the terahertz range (>1 THz) and the effective conductivity of the composite can be approximately found as a sum of the conductances of the inclusions in the unit volume with a factor 1/3 which takes into account the random orientation of the nanoparticles [36]. The conductivity of CNT and GNP films at 1 THz is 55 S/cm and 87 S/cm, respectively, i.e. it

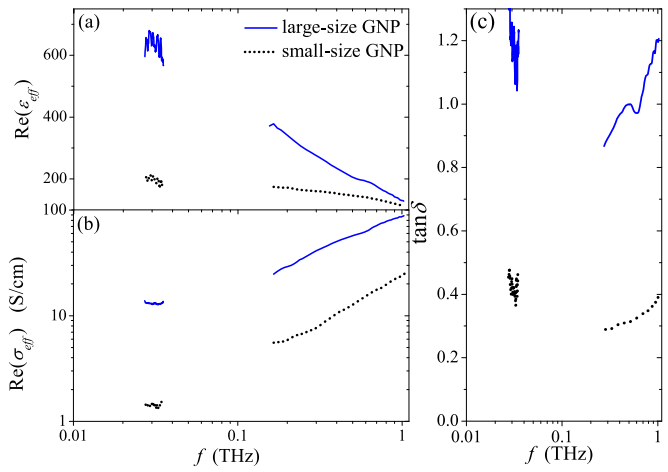

Figure 3. Frequency dependence of (a) Re(ε_{eff}), (b) Re(σ_{eff}) and (c) tan δ for films comprising large- and small-size GNPs.

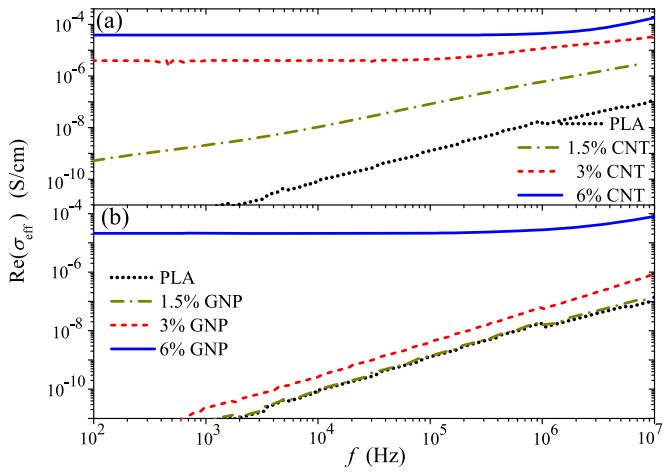

Figure 4. Frequency dependence of Re(σ_{eff}) for the (a) CNT/PLA and (b) GNP/PLA composites at different filler mass fractions 1.5, 3, and 6 wt%. Data for the PLA are shown by a dotted line.

is approximately of the same order. The same is observed for the GNP and CNT composites at the same loading. This means that roughly speaking, the quantity of quasi-free charges per unit volume is approximately identical for GNP and CNT samples at the same filler concentration. However, the microwave conductivities of GNP samples are much smaller than those of CNT samples at the same weight concentration of the inclusions (compare figures 5 and 6), i.e., the frequency dependence $\sigma_{\text{eff}}(f)$ is stronger for the GNP than for the CNT samples. The same difference between GNPs and CNTs has been reported in the range of 0.1–1.0 THz [40]. This can be explained by the fact that the GNPs are stronger isolated from one another than the CNTs, and consequently, the screening effect is stronger in the GNPs than in the CNTs. Stronger isolation may occur if the charge transport is hampered. For example, in the case of GNP, the electrons have to move along a conductive path which includes tunneling barriers not only between the adjacent graphene flacks but also between the layers of each multilayer flack.

Figures 7 and 8 show the values Re($\varepsilon_{\text{eff}} - \varepsilon_{\text{h}}$) and Re($\sigma_{\text{eff}} - \sigma_{\text{h}}$) versus weight concentration F of the fillers at different frequencies for CNT and GNP samples, respectively. Here, the effect of the dielectric matrix has been excluded by the subtraction of the permittivity ε_h and conductivity σ_h of the PLA. In order to show how the concentration dependence changes with frequency, the data in figures 7 and 8 were fitted with power-law formulas Re($\varepsilon_{\text{eff}} - \varepsilon_{\text{h}}$) $= AF^{\alpha}$, and Re($\sigma_{\text{eff}} - \sigma_{\text{h}}$) $= BF^{\beta}$. The exponents α and β at different frequencies are represented in figures 9(a), (b). At low frequencies, the screening effect is stronger providing stronger concentration dependence and consequently the larger value of the exponents β and α. Inequalities $\beta > 1$ and $\alpha > 1$ occur due to the effect of contacts—the screening effect becomes weaker when the number of interparticle contacts increases. The influence of contacts is stronger at lower frequencies, that is why the exponents decrease as frequency increases. In the terahertz range, the effect of contacts vanishes and the values of

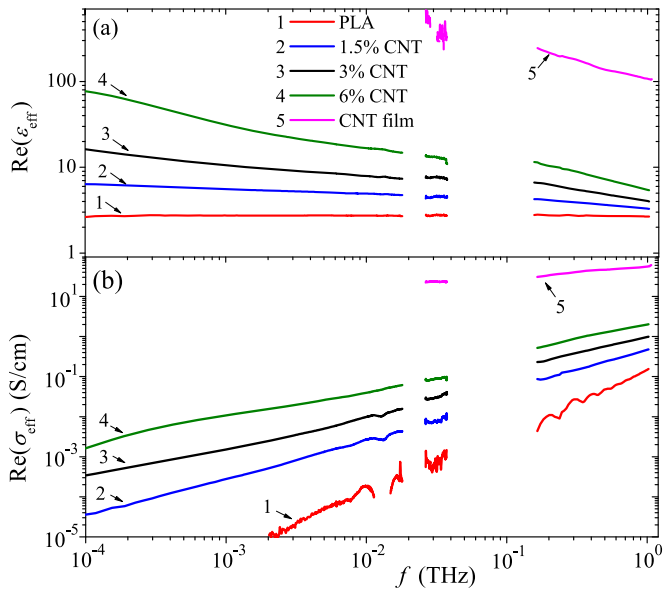

Figure 5. Frequency dependence of (a) Re(ε_{eff}) and (b) Re(σ_{eff}) for the CNT film, PLA, and CNT/PLA composites at different CNT mass fractions 1.5, 3, and 6 wt%.

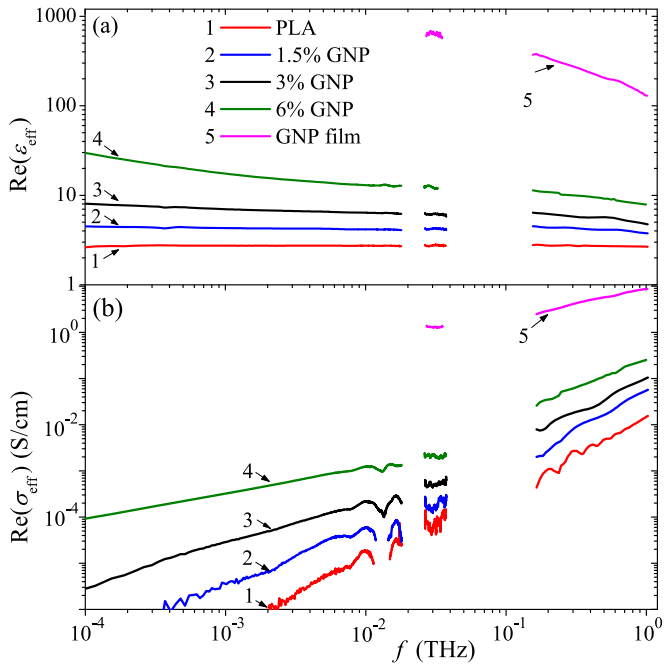

Figure 6. Frequency dependence of (a) Re(ε_{eff}) and (b) Re(σ_{eff}) for the GNP film, PLA, and GNP/PLA composites at different GNP mass fractions 1.5, 3, and 6 wt%.

β and α reach unity. The almost linear dependence of the composite conductivity on the mass fraction of nanoparticles in the terahertz range can be used for quantitative estimation of the filler density in the polymer matrix.

It should be noticed that the GNP samples at 1.5 and 3 wt% and CNT sample at 1.5 wt% are below the percolation threshold whereas other samples are above the percolation threshold (see their conductivities in table 1 and figure 4(a)). However, there is no any possibility to identify from spectra in figures 5–8 either the concentration of fillers is above or below the percolation threshold, i.e. the concentration dependence of the effective conductivity in static regime differs significantly from that in the microwave range [6, 13, 14]. Meanwhile, the dielectric loss tangent is rather sensitive to the percolation phenomena: it is much smaller than unity for composites below the percolation threshold. Figure 10 shows the frequency dependence of the value

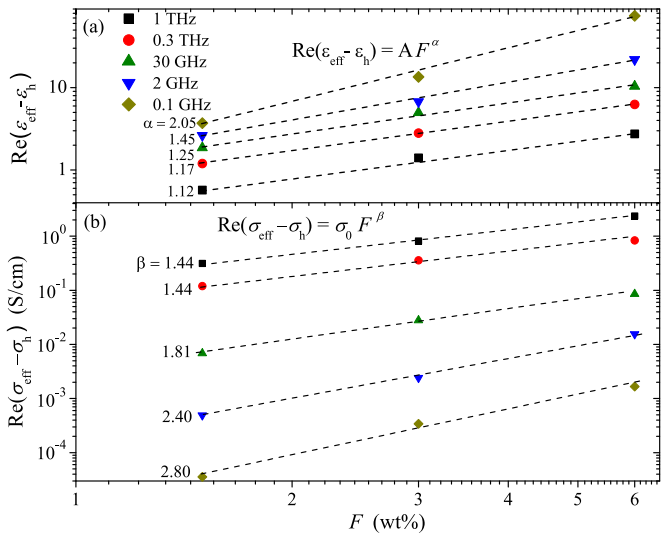

Figure 7. Contribution of CNTs to the permittivity and conductivity of CNT/PLA composites versus CNT mass fraction at different frequencies. The values (a) Re($\varepsilon_{\text{eff}} - \varepsilon_{\text{h}}$) and (b) Re($\sigma_{\text{eff}} - \sigma_{\text{h}}$) were obtained from figure 5, where ε_h and σ_h are parameters of the PLA matrix.

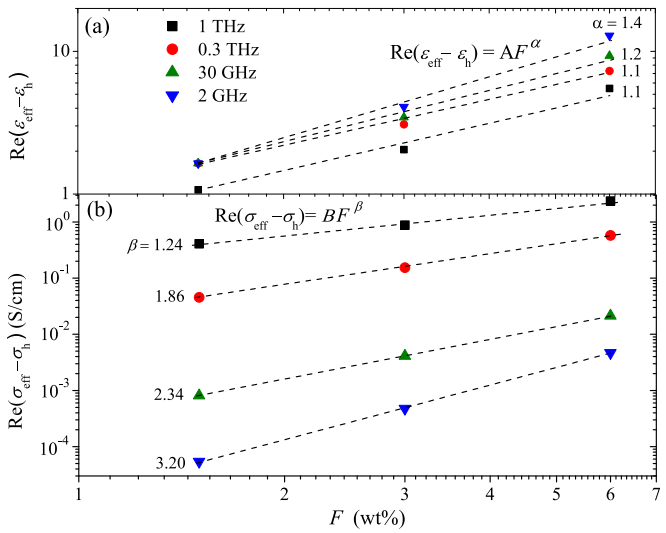

Figure 8. Contribution of GNPs to the permittivity and conductivity of GNP/PLA composites versus GNP mass fraction at different frequencies. The values (a) Re($\varepsilon_{\text{eff}} - \varepsilon_{\text{h}}$) and (b) Re($\sigma_{\text{eff}} - \sigma_{\text{h}}$) were obtained from figure 6, where ε_h and σ_h are parameters of the PLA matrix.

$\tan\delta = \text{Im}(\varepsilon_{\text{eff}} - \varepsilon_{\text{h}})/\text{Re}(\varepsilon_{\text{eff}} - \varepsilon_{\text{h}} + 1)$ for CNT and GNP films and composites. Here, we determined loss tangent in such a way to exclude from consideration the influence of the polymer matrix with the permittivity ε_h; it is supposed for the films that $\varepsilon_h = 1$. The value of tanδ is close to or larger than unity for CNT and GNP films as they perform a good conductive network. Moreover, the value of tanδ is larger for CNT than for GNP film indicating that interparticle electron transport is more effective in CNT than in GNP film. A very small value of the loss tangent for 1.5, 3 wt% GNP/PLA composites and for 1.5 wt% CNT/PLA composite in a wide range (1–36 GHz) is explained by the absence of the conductive network. For the concentrations above the percolation threshold (see 6 wt% GNP and 6 wt% CNT in figure 10), the loss tangent is rather high and it decreases with increasing frequency in the range 1–36 GHz and then increases in the range 0.2–1.0 THz.

To estimate the efficiency of inclusion interaction with the electromagnetic wave at specific frequency f, the following parameters are proposed for CNT composites [21]:

$$g(f, f_0) = \sigma_{\text{eff}}(f)/\sigma_{\text{eff}}(f_0), \quad (1)$$

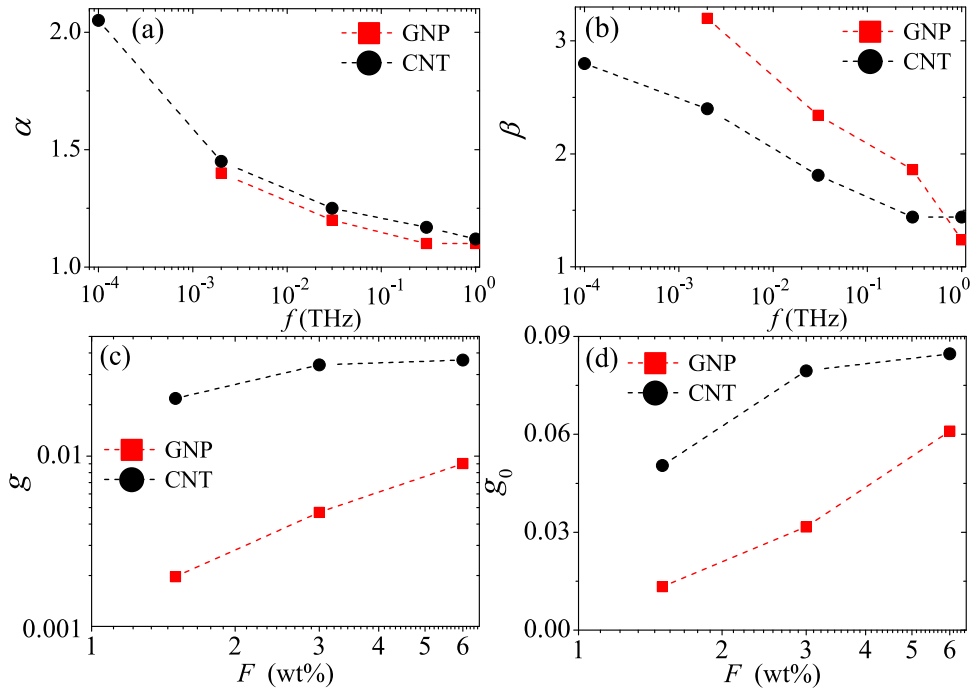

Figure 9. Frequency dependence of the exponents (a) α, and (b) β for GNP/PLA and CNT/PLA composites. They were found from fitting the data in figures 7 and 8 with the power-law formula. Parameters (c) g(30 GHz, 1 THz) and (d) g_0(30 GHz, 1 THz) versus the mass fraction of the inclusions for CNT/PLA and GNP/PLA composites.

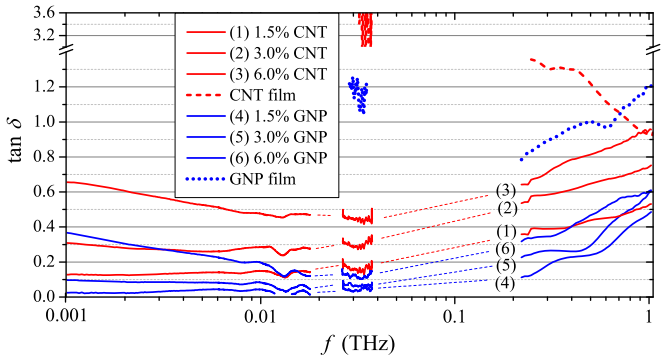

Figure 10. Frequency dependence of the dielectric loss tangent for CNT and GNP films and composites at different filler mass fractions 1.5, 3, and 6 wt%.

and

$$g_0(f, f_0) = g(f, f_0)/g_{film}(f, f_0), \tag{2}$$

where f_0 is a frequency, at which the screening effect vanishes and electromagnetic interaction is maximally possible. Further, for our estimations, we assume that $f_0 = 1$ THz for our samples. $g_{film}(f, f_0)$ is the parameter g for a pure film containing the very same kind of nanoparticles as the composite material does. Since the maximal electromagnetic interaction with fillers occurs when they are densely packed forming a thin film, one can consider this film as a perfect composite with maximal possible parameter g. As the mechanism of the electromagnetic interaction is the same both for CNTs and GNPs, the parameters g and g_0 can be applied for the characterization of GNP based composite as well.

Figures 9(c), (d) shows the parameters g and g_0 at 30 GHz for CNT and GNP samples versus the weight concentration of nanoparticles. As shown in figure 9(c), the parameter g for CNT samples is 0.01–0.02 meaning that, roughly speaking, only 1%–2% of the charge carriers contribute to the electromagnetic response of the composite, whereas other charge carriers are screened. For GNP samples, the parameter g is 4–10 times less than for CNT samples and it depends strongly on the filler concentration. Thus, in spite of the similar intrinsic conductivity of the GNP and CNT, the latter interacts more effectively with the microwave radiation. The

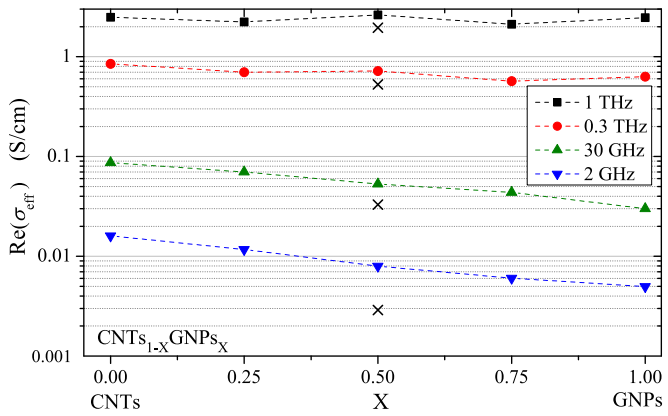

Figure 11. Effective conductivity of the GNP/CNT/PLA composites versus the relative mass content of GNPs X at total filler content 6 wt% and different frequencies. Cross symbols indicate the sum of the conductivities of 3 wt% GNP and 3 wt% CNT composites at different frequencies: 1 THz, 0.3 THz, 30 GHz, and 2 GHz from up to down.

parameter g_0 at 30 GHz is between 0.02 and 0.09 (see figure 9(d)) meaning that the efficiency of the filler interaction with the electromagnetic field is 2%–9% in comparison with that for the films.

Figure 11 shows the real part of the effective conductivity of the bi-filler GNP/CNT polymer composites versus the relative content of GNP X at total filler content 6 wt% and different frequencies. One can see from figure 11 that the effective conductivity at 1 THz practically does not depend on X providing confirmation that (i) the terahertz conductivity of our samples is determined by the intrinsic conductivity of our fillers, and (ii) the number of free-charge carriers per unit mass of nanofillers is the same for the GNP and CNT materials. The dependence $\mathrm{Re}(\sigma_{\mathrm{eff}})$ on X becomes stronger as frequency decreases. This is in agreement with our outcome that the microwave field interacts with the CNTs more effectively than with the GNPs.

One may say about a synergistic effect if the co-contribution of two types of fillers to the conductivity is more than the sum of individual filler's contributions [41]. Cross symbols in figure 11 indicate the sum of the conductivities of 3 wt% GNP and 3 wt% CNT composites at different frequencies. Comparing them with the conductivity of bi-filler composite at $X = 0.5$, we may say that the synergy effect occurs in the bi-filler samples. This effect is weak in the terahertz range, where the conductivity of the bi-filler sample almost coincides with the sum of the conductivities of the one-filler samples, whereas it is strong at 2 GHz where the difference in the conductivities appears to be 2.6 times. There are two possible reasons of the synergy effect: (i) fillers of one type can improve the dispersion of the fillers of another type, and (ii) the electrical contacts between fillers of different types lead to additional conducting pathways in the composite and consequently to a weakening of the screening effect.

Let us notice that our results are in agreement with [41–44] where a synergistic effect in the enhancement of electrical properties and electromagnetic interference shielding response for hybrid GNP/CNT polymer composites and forms has been demonstrated.

3. Conclusion

The frequency and filler density dependencies of the effective conductivity of polymer composites with CNTs and GNPs embedded have been measured, compared and analyzed in the microwave and terahertz frequency ranges. We explain the observed strong frequency dependence of the conductivity by the screening effect both in individual nanoparticles and their agglomerates. This effect is strong at low frequencies and rather weak in the terahertz range.

We have shown that the density dependencies can be fitted with the power-law formulas with frequency dependent exponents being about 3 at 100 MHz and about 1 at 1 THz when mass fraction varies in the range from 1.5 to 6 wt%. Though this range includes the percolation threshold, there are no so strong changes in the effective conductivity of the composites as it happens in the static regime. As the terahertz effective conductivity is almost proportional to the concentration of nanofillers, it can be used for the estimation of the filler concentration.

Thin films made of CNTs or GNPs were proposed to consider as 'perfect' composites with respect to their electromagnetic interaction. It is reasonable to compare their parameters with those of the composites. The ratio of the microwave to terahertz effective conductivities is proposed for the estimation of the efficacy of the

electromagnetic interaction of GNPs within the GNP-based composite. The application of this ratio to CNT-based composite has been recently justified in [21].

Synergy effect in the enhancement of the effective conductivity is demonstrated for the composite comprising a mixture of CNTs and GNPs. This effect is weak in the terahertz range and becomes stronger as frequency decreases.

Acknowledgments

This research was partially supported by the Belarusian Republican Foundation for Fundamental Research (BRFFR) project F18Kor-002. The work has also benefited of funding from the EU H2020 program under the MSCA-RISE-2016 project 734164 'Graphene-3D'. MVS, DSB, PPK, and SAM are thankful for support by Tomsk State University Competitiveness Improvement Program. PK is thankful to the Grant of the President of the Republic of Belarus in science, education, health, and culture in 2019.

ORCID iDs

M V Shuba https://orcid.org/0000-0003-4828-7242
D Meisak https://orcid.org/0000-0002-6249-2181

References

[1] Stauffer D and Aharony A 1992 *Introduction to Percolation Theory* (London: Taylor and Francis)
[2] Ambrosetti G, Grimaldi C, Balberg I, Maeder T, Danani A and Ryser P 2010 *Phys. Rev.* B **81** 155434
[3] Plyushch A, Lamberti P, Spinelli G, Macutkevič J and Kuzhir P 2018 *Appl. Sci.* **8** 882
[4] Bauhofer W and Kovacs J Z 2009 *Comp. Sci. Techn.* **69** 1486–98
[5] Qin F and Brosseau C 2012 *J. Appl. Phys.* **111** 061301
[6] Andreev A S, Kazakova M A, Ishchenko A V, Selyutin A G, Lapina O B, Kuznetsov V L and d'Espinose de Lacaillerie J B 2017 *Carbon* **114** 39–49
[7] Sun X, Sun H, Li H and Peng H 2013 *Adv. Mater.* **25** 5153–76
[8] Meng F, Wang H, Huang F, Guo Y, Wang Z, Hui D and Zhou Z 2018 *Composites Part B: Engineering* **137** 260–77
[9] Kashi S, Hadigheh S A and Varley R 2018 *Polymers* **10** 582
[10] Kuzhir P *et al* 2011 *Thin Solid Films* **519** 4114–8
[11] Stankovich S, Dikin D A, Dommett G H B, Kohlhaas K M, Zimney E J, Stach E A, Piner R D, Nguyen S T and Ruoff R S 2006 *Nature* **442** 282
[12] Sandler J, Kirk J, Kinloch I, Shaffer M and Windle A 2003 *Polymer* **44** 5893–9
[13] Kranauskaite I, Macutkevic J, Banys J, Kuznetsov V L, Moseenkov S I, Rudyna N A and Krasnikov D V 2016 *Phys. Stat. Sol. (a)* **213** 1025–33
[14] Plyushch A, Macutkevic J, Kuzhir P, Banys J, Bychanok D, Lambin P, Bistarelli S, Cataldo A, Micciulla F and Bellucci S 2016 *Compos. Sci. Technol.* **128** 75–83
[15] Slepyan G Y, Maksimenko S A, Lakhtakia A, Yevtushenko O and Gusakov A V 1999 *Phys. Rev.* B **60** 17136–49
[16] Sule N, Willis K J, Hagness S C and Knezevic I 2014 *Phys. Rev.* B **90** 045431
[17] Karlsen P *et al* 2017 *J. Phys. D: Appl. Phys.* **51** 014003
[18] Gorshunov B *et al* 2018 *Carbon* **126** 544–51
[19] Hong J T, Lee K M, Son B H, Park S J, Park D J, Park J Y, Lee S and Ahn Y H 2013 *Opt. Express* **21** 7633–40
[20] Shuba M V, Melnikov A V, Paddubskaya A G, Kuzhir P P, Maksimenko S A and Thomsen C 2013 *Phys. Rev.* B **88** 045436
[21] Shuba M, Yuko D, Kuzhir P, Maksimenko S, Kanygin M, Okotrub A, Tenne R and Lambin P 2018 *Carbon* **129** 688–94
[22] Shuba M V, Slepyan G Y, Maksimenko S A and Hanson G W 2010 *J. Appl. Phys.* **108** 114302
[23] Shuba M V, Yuko D I, Kuzhir P P, Maksimenko S A, Crescenzi M D and Scarselli M 2018 *Nanotechnology* **29** 375202
[24] Peters O, Busch S F, Fischer B M and Koch M 2012 *Int. J. Infr. Mill. Waves* **33** 1221–6
[25] Egiziano L, Lamberti P, Spinelli G, Tucci V, Kotsilkova R, Tabakova S, Ivanov E, Silvestre C and Di Maio R 2018 *AIP Conf. Proc.* **1981** 020152
[26] Skalsky S, Molloy J, Naftaly M, Sainsbury T and Paton K R 2018 *Nanotechnology* **30** 025709
[27] Spinelli G *et al* 2018 *Materials* **11** 2256
[28] Batakliev T *et al* 2019 *Appl. Sci.* **9** 469
[29] Hennrich F, Lebedkin S, Malik S, Tracy J, Barczewski M, Rosner H and Kappes M 2002 *Phys. Chem. Chem. Phys.* **4** 2273–7
[30] Zak A, Sallacan-Eecker L, Margolin A, Genut M and Tenne R 2009 *Nano* **04** 91–8
[31] Paddubskaya A *et al* 2016 *J. Appl. Phys.* **119** 135102
[32] Chung B K 2007 *Progress In Electromagnetics Research* **75** 239
[33] Hennrich F, Krupke R, Arnold K, Rojas Stütz J A, Lebedkin S, Koch T, Schimmel T and Kappes M M 2007 *J. Phys. Chem.* B **111** 1932–7
[34] Thomsen C and Reich S 2007 *Top. Appl. Phys.* **108** 115–234
[35] Shuba M V, Paddubskaya A G, Kuzhir P P, Maksimenko S A, Flahaut E, Fierro V, Celzard A and Valusis G 2017 *J. Phys. D: Appl. Phys.* **50** 08LT01
[36] Slepyan G Y, Shuba M V, Maksimenko S A, Thomsen C and Lakhtakia A 2010 *Phys. Rev.* B **81** 205423
[37] Sarto M S, D'Aloia A G, Tamburrano A and Bellis G D 2012 *IEEE Trans. Electromagn. Compat.* **54** 17–27
[38] Marra F, D'Aloia A G, Tamburrano A, Ochando I M, De Bellis G, Ellis G and Sarto M S 2016 *Polymers* **8** 272
[39] Bychanok D *et al* 2018 *J. Phys. D: Appl. Phys.* **51** 145307
[40] Jung G B *et al* 2010 *J. Phys. Chem.* C **114** 11258–65

[41] Zhang H, Zhang G, Tang M, Zhou L, Li J, Fan X, Shi X and Qin J 2018 *Chem. Eng. J.* **353** 381–93
[42] Verma M, Chauhan S S, Dhawan S and Choudhary V 2017 *Composites Part B: Engineering* **120** 118–27
[43] Perets Y, Aleksandrovych L, Melnychenko M, Lazarenko O, Vovchenko L and Matzui L 2017 *Nanoscale Res. Lett.* **12** 406
[44] Melnychenko M, Perets Y, Aleksandrovych L, Vovchenko L L, Lazarenko O and Matzui L 2017 Dielectric properties of nanocarbon polymer composites with binary filler *Nanophysics, Nanomaterials, Interface Studies, and Applications. NANO 2016. Springer Proceedings in Physics* vol 195 (Berlin: Springer) (https://doi.org/ 10.1007/978-3-319-56422-7_66)